The Mechanical Roles of Chaperons

Deep Chaudhuri[#], Souradeep Banerjee[#], Soham Chakraborty, Shubhasis Halder*

Department of Biological Sciences, Ashoka University, Sonepat, Haryana 131029

# contributed equally to this work

*to whom correspondence may be addressed. Email- shubhasis.halder@ashoka.edu.in

Abstract

Protein folding under force is an integral source of generating mechanical power to carry out diverse cellular functions. Though chaperones interact with proteins throughout the different stages of folding pathways, how they behave and interact with client proteins under force was not known.

Here we introduce the 'mechanical role' of chaperone and explained it with seven independent chaperones using single molecule based real-time microfluidics-magnetic-tweezers. We showed and quantified how chaperones increase or decrease mechanical work output by shifting the folding energy landscape of the client proteins towards the folded or unfolded state. Notably, we found chaperones could behave differently under force. For instance: trigger factor, ribosomal-tunnel associated chaperone, working as a holdase in absence of force, but assist folding under force. This phenomenon generates extra mechanical energy to pull the polyprotein from the stalled ribosome. This is also relevant for SecYEG tunnel associated oxidoreductase DsbA, which act similarly like TF and increases the mechanical energy up to ~59 zJ, to facilitate membrane translocation in an energy efficient manner. However cytoplasmic oxidoreductases such as PDI and Thioredoxin, unlike DsbA, do not have the mechanical folding ability. Interestingly, we observed a highly potential foldase-DnaKJE chaperone complex, only restores the folding ability of the client protein and fails to act like TF or DsbA under force. However, the individual components of this complex, DnaK or DnaJ, act as a mechanical holdase and inhibits folding; similar to that of SecB. Together our study provides an emerging insight of mechanical chaperone behavior, where tunnel associated chaperones generate extra mechanical work whereas the cytoplasmic chaperones are unable to generate that, which might have evolved to minimize the energy consumption in biological processes.

Introduction:

Protein folding under force is an important source of generating mechanical energy that harnesses different biological functions ranging from protein translation to degradation [1–4]. For example, in translation, protein synthesis occurs in confined ribosomal tunnel under 7-11 pN force while ClpX machinery generates 4-15 pN force to unfold protein followed by ClpP dependent degradation [2,5,6]. In between translation and degradation, protein folding under force generates mechanical work which is important for delivering mechanical energy during various processes [1–4]. Though chaperones are well known for their assisting role in folding [7–11], it is not known how chaperones interact under force and modulate the mechanical work to regulate cellular energy consumption.

To address this question, we investigated the mechanical role of different chaperones and chaperone-like proteins under force, individually and in combinations: DnaK, DnaJ, SecB, DsbA, Trigger factor (TF), protein disulfide isomerase (PDI) and thioredoxin (Trx). The mechanical effects of these chaperones were monitored by our novel real-time microfluidic-magnetic-tweezers (RT-MMT) that implements both force clamp and force ramp technology [12]. Using the force clamp technology constant force can be provided on a protein, offering a unique way to probe both thermodynamics and kinetic properties of the chaperone-protein interactions under equilibrium condition. Whereas, the force ramp technology, by increasing or decreasing the force at constant velocity, detects unfolding and refolding interactions during the process. Furthermore, the advantage of broad force ranges from 0 to 120 pN, with sub-pN resolution, allows us to monitor the effect of chaperone on both the folded and unfolded states of the substrate independently. Moreover, the associated microfluidics system offers multiple injections of different chaperones, one by one or in combination, and tracking their dynamic changes on a single client protein molecule in real time. Lastly, using this technology, the force can be precisely applied on the substrate protein while keeping the chaperone unperturbed.

Our results showed that chaperones behave differently under force than their known role. Prototypical chaperone TF, having a well-known holdase function in absence of force [13,14], behaves differently under force by accelerating refolding kinetics and generates a mechanical work of 59.5 zJ. A distinct property is also observed for DnaKJE (DnaK+DnaJ+GrpE+ATP) complex under force. In absence of force, this complex work as a typical foldase [15–19]; but in presence of force, it only restores the intrinsic folding ability of proteins. Similar to TF,

another tunnel associated oxidoreductase enzyme DsbA, increases the mechanical work output to two-fold by assisting protein folding under force that reduces the energy consumption by SecA motor. In contrast, other cytosolic oxidoreductase enzymes such as, PDI and Trx are not able to accelerate the protein folding like DsbA and exhibit only the restoring activity under force. However, DnaK, DnaJ, SecB chaperones, both in absence and presence of force, function as holdase and reduce the mechanical work by hindering the folding process. Thus, we reclassified the chaperones into three classes on the basis of their mechanical characteristics: mechanical unfoldase including, DnaJ, DnaK, and SecB; mechanical restorase such as, DnaKJE, PDI and Trx and lastly, mechanical foldase such as, TF and DsbA. Chaperones associated with tunnels, TF and DsbA possess a special mechanical activity under force by which they can generate extra mechanical power to pull protein from ribosome to cytoplasm and cytoplasm to periplasm. By contrast, the same proteins, in absence of force, behaves as a holdase. Overall, these data reconcile that chaperone, by modifying free energy landscape of substrate proteins, generates the mechanical power that provides a distinct view of mechanical folding pathway of proteins under equilibrium.

Results and Discussions:

Real time measurements of single protein folding by microfluidic magnetic tweezers:

The combination of microfluidic system with a covalently linked magnetic tweezers allow us to probe the folding-unfolding dynamics of a single protein in presence of chaperone where the force can only be applied on the proteins while chaperones remain unaffected. Additionally, the force can be precisely controlled in sub-pN resolution that allows us to observe the dynamic folding-unfolding transition in polyprotein, providing information in equilibrium. We performed the experiment on an engineered construct containing eight repeats of protein L B1 domain, inserted between N terminus HaloTag and C terminus AviTag. The polyprotein is tethered on glass surface by covalent HaloTag chemistry and attached to the paramagnetic beads by biotin streptavidin-biotin chemistry. Applied force on paramagnetic beads is regulated by a pair of permanent magnets, attached to the voice coil actuator. The force is determined as an inverse function of distance between paramagnetic beads and permanent magnets [20]. The force magnitude can be calibrated by changing the magnet-beads distance such as, moving down the magnet position from 4.0 mm to 1.3 mm results in an increase in force pulse from 4.3 pN to 45 pN (Fig. 1A). The unfolding high pulse

at 45 pN unfolds the domains which are observed as increase in step size (described as difference in length between folded and unfolded domain).

Fig. 1B demonstrates the representative folding trajectory obtained by our single molecule experiment that consists of two phases: at first, the polyprotein is unfolded at 45 pN to generate eight discrete stepwise extensions as a single molecule fingerprint and subsequently reduced to a equilibrium force of 8 pN where any changes in folding-unfolding dynamics can be precisely monitored as upward steps of unfolding and downward steps of refolding. The unfolding trajectory is magnified in the inset of Fig. 1B where the first passage time (FPT) of unfolding is denoted as-minimum time leading to complete unfolding of eight domains from fully folded state and similarly for FPT of refolding, time taken to complete refolding of all domains from fully unfolded state. Mean-FPT (MFPT) is calculated by averaging the FPT values over numerous trajectories, providing a model-free metric that describes unfolding and refolding kinetics of proteins under force.

We determined the folding probability by dwell-time analysis from equilibrium phases over many folding trajectories (Fig. 1B). Along the equilibrium phase, each folded state is named as I (number of folded state) and their residence time along the phase is determined as $t = T_I/T_t$, where T_I is the duration of I state and $T_t = \sum_I T_I$, total observable duration of the equilibrium phase (Supplementary Figure. 1). FP is calculated as normalized averaged state (Supplementary Table. 1),

$$FP = \sum_I I \times t/N \qquad (1)$$

Where, N is defined as numbers of total domains. Detailed calculations of folding probability have been explained in supplementary information, whereas the free energy of refolding under equilibrium can be classified in equation 2.

$$\Delta G_{U\to F} = -\ln \frac{FP}{(1-FP)} \qquad (2)$$

Protein L does not form misfolded state under force:

The chaperone mechanisms are mostly studied with the substrate proteins which are prone to form misfolded state and aggregation [16,17,21,22]. To eliminate these diverse conformational dynamics, we used well-known protein L B1 domain that has been reported to exhibit distinct folding-unfolding dynamics without misfolded or intermediate states under equilibrium condition [13,20,23–25]. Here, we used a continuous force ramp technology to detect the presence of any misfolded state in a force dependent process (Fig. 2). We increased the mechanical force at a constant rate of 2.53 pN/s which promotes mechanical unfolding of the substrate

protein. By using an octamer protein L construct, we observed unambiguous eight step sizes in each unfolding pulse. Our result shows the mechanical strength of protein does not change with the unfolding and refolding pulses, indicating the absence of misfolded state (Fig. 2B). Additionally, presence of eight discrete steps in each pulse eliminates the possibility of any intermediate state during the folding or unfolding pathway (Supplementary Figure. 1-6, 9-10).

DnaJ induces mechanical unfolding and suppresses refolding:

DnaJ is a prototypical chaperone that holds the polypeptide from trigger factor and then, either transfers it to SecA for translocation or fold with the help of DnaK/DnaJ/GrpE [26–29]. Here, we test the mechanical activity of DnaJ using protein L as substrate protein. Fig. 3A describes the variation in MFPT of refolding as a function of force in both absence (black) and presence of 1 μM DnaJ (red). The MFPT of refolding steadily increases with force magnitude, however, at a particular force with DnaJ, the MFPT of refolding is higher than without DnaJ such as, at 5 pN in absence of DnaJ, the polyprotein requires 6.3±2.03 s for complete refolding but with DnaJ, it increases to 25.43±0 s. In case of unfolding kinetics, the presence of DnaJ (red) decreases the MFPT of unfolding than that observed in absence of DnaJ (black). At 44 pN without DnaJ, the polyprotein requires 24.6±3.1 s to completely unfold while it reduces to only 10.4±3.6 s in presence of DnaJ (Fig. 3B). Thus, DnaJ accelerates the unfolding kinetics and retards the refolding kinetics.

To study the effect of DnaJ on the folding probability, we measured folding probability (FP) as a function of force and compared it with the control (black) and presence of DnaJ (red) (Fig. 3C). Folding probability decreases with increasing force, indicating an inverse relation of protein folding with force. However, adding DnaJ, impedes the protein folding and thus, decreases the folding probability. At 4 pN, the folding ability of the polyprotein is almost 100% and thus, FP=1, irrespective to the presence of DnaJ and at 10 pN, the FP becomes zero. Interestingly, it is the intermediate force range of 5-9 pN where the profound reduction in folding probability is observed in presence of DnaJ and the difference in probability becomes highest in 8 pN. At 8 pN without DnaJ, the FP is 0.51 whereas it decreases to only 0.17 in presence of DnaJ (Supplementary Figure. 2). Additionally, the Half-point force (defined as force where FP is 0.5) has been observed to shift from 8 pN to ~6.9 pN which suggest a lower refolding ability in presence of DnaJ. The equilibrium free energy for the mechanical folding has been determined from the folding probability at constant force of 8 pN. We calculated the free energy in absence of DnaJ is -0.04 kT and that in presence of

DnaJ is +1.58 kT (equation 1 and 2). Similarly, at 7 pN, in absence of DnaJ the free energy is -1.26 kT and in presence of DnaJ is +0.16 kT. These results collectively suggest that DnaJ redesigns the energy landscape towards the unfolded state. Moreover, the acceleration of unfolding kinetics and delaying the refolding kinetics implies the capability of DnaJ to destabilize the folded state of protein L while stabilizing the unfolded state (Fig. 3D).

DnaK prevents the protein L refolding under force:

DnaK, in absence of force, shows the holdase property where it reduces the rate of refolding of its client protein [14,15,30–32]. Thus, to understand the effect of DnaK in mechanically induced equilibrium, we studied the kinetics and equilibrium properties of protein L in presence of 3 μM DnaK. Fig. 4A and 4B demonstrate the comparisons in MFPT of refolding and unfolding in presence (red) and absence of DnaK (black) as a function of force. DnaK decreases the refolding kinetics and increasing unfolding kinetics of proteinL.

Fig. 4C illustrates the equilibrium properties of protein L folding in absence (black) and presence of DnaK (red) within the range from 4-11 pN. Analogous to DnaJ, DnaK also decreased the folding probability in the intermediate force range of 5-9 pN while the folding probability remained unchanged in two extreme forces. As an instance, at 8 pN without DnaK, the FP is 0.51 while it reduces to 0.22 in presence of DnaK, suggesting a ~44% reduction in folding probability (Supplementary Figure. 3). From the folding probability, we calculated the free energy in both the conditions as previously mentioned in eq. 2. The presence of DnaK, at 8 pN, increases the equilibrium free energy from -0.04 to +1.26 kT, inclining the energy landscape towards the unfolded state (Fig. 4D). Similar result has also been observed at 9 pN, where the free energy changes from +1.81 kT in absence of DnaK to +2.71 kT in presence of DnaK. These data reconcile that at equilibrium force conditions, DnaK compromises the refolding ability in protein L and prevents their premature misfolding.

The Synergistic action of DnaKJE restores the mechanical refolding efficiency in protein L:

So far, the experiments performed showed that individually DnaJ and DnaK chaperones significantly decrease the refolding ability of the substrate protein L under force. We therefore asked whether the complete chaperone complex (comprised of DnaK, DnaJ, GrpE and ATP) restores the mechanical refolding efficiency in protein or not. To systematically explore that, we unfolded and refolded the protein L octamer in presence of chaperone

complex (1 µM DnaJ+3 µM DnaK+5 µM GrpE+5 mM ATP) and compared that with the DnaJ activity. The MFPT-refolding decreases in presence of the chaperone complex (red) than only in DnaJ (black) (Fig. 5A). This suggests a higher refolding yield of protein L which is also apparent from folding probability where a rightward shift has been observed during the refolding experiment with the addition of entire chaperone complex in buffer (Fig. 5C and Supplementary Figure. 4). Similarly, in unfolding kinetics, the total unfolding time is higher in DnaK complex (red) than DnaJ (black), representing a slower unfolding kinetics in presence of chaperone complex (Fig. 5B). Furthermore, the effect of the DnaJ/DnaK/GrpE complex is evident in mechanical folding landscape where it reverts the landscape by stabilizing the folded state and destabilizing the unfolded state (Fig. 5D). In summary, these data nicely demonstrate that chaperoning by whole DnaJ/DnaK/GrpE complex promotes folding by increasing refolding efficiency in protein L.

SecB acts as mechanical unfoldase:

SecB is a well-known chaperone to bind molten globule state and thus delay the formation of stable tertiary contacts [33,34]. Fig. 6A and 6B shows, SecB (3µM) slows down the refolding kinetics and increases the unfolding kinetics of protein L. For instance, at 6 pN, MFPT-refolding increases from 21.8±5.1 s (without SecB, black) to 42.47±1.24 s in the presence of SecB (red) (Fig. 6A) whereas the MFPT for unfolding, at 44 pN, reduces from 24.6±3.1s (without SecB, black) to 17.46±2.51s (with SecB) (Fig. 6B). Fig. 6C compares the folding probability with (red) and without SecB (black): similar to DnaJ-DnaK system, at any force within the intermediate range, the folding probability substantially decreases in presence of SecB (Supplementary Figure. 5) and, the half-point force is decreased from 8 pN to 7.17 pN. The decreased refolding kinetics and folding probability suggested that SecB redesigns the folding landscape by reducing the stability of the folded state and increasing the stability of the unfolded state (Fig. 6D).

Mechanical foldase activity of DsbA:

The periplasmic oxidoreductase enzyme DsbA has a well characterized function to transfer the disulfide bond to substrate proteins by reducing its catalytic *CXXC* motif and helps in folding of cysteine containing proteins [35–39]. Interestingly, few studies revealed the role of DsbA in transporting of cysteine free proteins through translocon pore, suggesting its plausible chaperone activity independent to oxidoreductase activity [36,40]. Therefore, we

explore the mechanical chaperone activity of DsbA by using our substrate protein L, a cysteine free globular protein. Unlike DnaJ or SecB, the refolding kinetics is greatly increased in presence of DsbA while slight change was observed in unfolding kinetics (Fig. 7A and 7B). At a given force, an efficient folding ability in proteins has been observed in presence of DsbA (Fig. 7C and Supplementary Figure. 6) and the most profound effect is observed at 9 pN force. From the folding probability and MFPT calculations, we found that DsbA completely tilts the folding landscape towards the folded state by destabilizing the unfolded state and slightly stabilizing the folded state (Fig. 7D). This finding is consistent with accelerated protein folding process under force by DsbA assistance.

Mechanical chaperone activity of thioredoxin domain containing proteins:

DsbA, possessing a *CXXC* motif (thioredoxin domain), shows a strong chaperone activity, which led us to further investigate whether this phenomenon is generalized to all thioredoxin domain containing proteins. We test two independent oxidoreductase proteins: full length PDI and Trx. Though PDI and Trx have been shown to restore the intrinsic folding, they are unable to show extra mechanical folding behavior as observed in presence of DsbA (Fig. 8; Supplementary Figure. 9 and 10). This concludes that tunnel associated thioredoxin proteins like DsbA has a special mechanical activity by which they generate extra mechanical power to help the shipment of proteins from cytoplasm to periplasmic side.

Comparative analysis of chaperone activity on a single proteinL:

We represented a comparative analysis of how mechanical chaperones modulate the energy landscape and folding dynamics on a single protein L under equilibrium force condition at 8 pN (Fig. 9). In absence of chaperones, the polyprotein hops between its 4^{th} and 5^{th} folded state, generating a folding probability of approx. 0.5 (black, Fig. 9A). Further addition of mechanical chaperones shifts this folding transition either towards folded state or unfolded state. For example, in presence of DnaJ the same polyprotein hops between its 1^{st} and 2^{nd} folded state (red trace, Fig. 9A) while addition of DsbA, increases this intrinsic folding ability to show a folding-unfolding transition between the 6^{th}, 7^{th} and 8^{th} folded states, (blue, Fig. 9A). We compared the folding probability as a function of force with different chaperones as shown in Fig. 9B. In presence of mechanical foldase chaperones such as, TF and DsbA, a rightward shift in folding probability is observed, representing a higher refolding yield in polyprotein whereas in presence of other chaperones like DnaJ, DnaK and SecB, the half-point force is shifted towards the lower force regime, suggesting a compromised ability of

proteins to remain folded under force. Indeed, these results collectively suggest the chaperones tilts the equilibrium folding landscape by modulating the intrinsic ability of protein folding under force.

Protein folding against the force generates mechanical work, for instance, titin protein produces 105 zJ of mechanical work during muscle contraction [3]. We found the mechanical energy can heavily be altered by chaperones by shifting the energy landscape either to the folded or unfolded state. The mechanical work can be calculated by multiplying the applied force with the mean step sizes and the folding probability under that particular force. Although chaperones could not influence the step size of proteinL, it largely affects the folding probability (Supplementary Figure 7 and Fig. 9B). In case of mechanical foldase chaperones (like TF or DsbA), the work output is maximum while it is minimum for the holdase chaperones (like DnaJ, DnaK or SecB) (Fig. 9C and Supplymentary Figure 8).

Discussion:

Protein folding under force is a significant source of delivering the mechanical power to carry out different cellular processes, but very less is known what further regulates the power output to maintain energy requirements [3,41–44]. Although the chaperones are of central importance in many biological phenomena, how they function and interact under force remains poorly understood. Our results show an empiric evidence and measurement that chaperones are able to generate mechanical work while assisting or hindering protein folding under high mechanical loads.

Our single molecule experiments, using force clamp technology, provided a force-induced equilibrium condition, which revealed an additional question about the thermodynamics of mechanical folding pathways: How are the chaperones able to reshape the energy landscape? A possible explanation is protein shows intrinsic folding-unfolding transitions under equilibrium, where force acting as denaturant tilts the equilibrium free energy landscape towards the unfolded state. Chaperones, known to assist protein folding in multiple ways, most likely reshapes the mechanical folding dynamics either by shifting the transition towards folded or unfolded state. Therefore, we used protein L which exhibits folded and unfolded states without any intermediate or misfolded structure (Fig 2), allowing distinct thermodynamic and kinetic effects of the chaperones on the energy landscape [13,20,23–25]. Unfoldase chaperones such as, DnaJ, DnaK and SecB have been observed to largely stabilize the unfolded state while greatly destabilizing the folded state and thus, reduces the folding

probability. In contrast to DnaJ/DnaK/GrpE chaperone complex, TF and DsbA have been observed to favor the refolding transitions under tension and show a more negative free energy towards the folded states. Moreover, shallow groove of unfolded state in the presence of these chaperones coincides with lower mechanical energy barrier that requires less energy and time to cross before spontaneous folding occurs.

It is well established that proteins fold under force and thus chaperone, already known to play a key role in assisting proper folding of protein through different mechanisms, might exhibit a force dependent activity. Here, we demonstrated chaperones could behave differently under force while interacting with substrate proteins. Such as TF, in absence of force, known to reduce folding rate and thus functions as holdase [13,14]. However, under force, it accelerates the refolding kinetics of substrate proteins and generates a pulling force upto 4 pN that helps to pull out the polypeptide from the stalled ribosome [13]. Interestingly, while applying zero force our result is consistent to previously observed results that TF reduces the folding efficiency. This answers a longstanding question of why in cell, TF maintains two states- ribosome bound and free cytosolic state. A rational interpretation is that the ribosome bound TF, working as mechanical foldase, generate a mechanical power to pull the protein from confined ribosomal tunnel while the free cytosolic state only behaves as holdase, slows down the refolding rate for efficient folding. Similarly, we have shown an oxidoreductase enzyme DsbA, associated with periplasmic mouth of SecYEG tunnel, speeds up the folding of translocating polypeptide which experiences a force of 7-11 pN in the SecYEG pore [5,45]. This acceleration in protein folding generates an excess mechanical work which reduces one third of the energy consumption for translocation along with increasing the translocation velocity. However, other oxidoreductase enzymes, PDI and Trx, didn't show the extra mechanical activity like DsbA. Similarly, cytoplasmic DnaKJE complex, in presence of force, has been observed to only restore the folding efficiency however, efficiently assist the folding in absence of force [9,15–17]. Thus, our study reveals an emerging concept of spatially distributed mechanical behavior of chaperone, where the tunnel associated chaperones generates extra mechanical energy while the cytoplasmic counterparts fails to do so. This may have evolved to minimize the energy consumption during various biological phenomenon where protein folds under force.

Our experimental finding provides a global mechanical activity of chaperones in diverse protein folding pathways: starting from emerging out of the ribosome to getting localized in its destined cellular region. Throughout this pathway, the nascent polypeptides interact with several chaperones and TF is the first one. It interacts with the polypeptide while

experiencing a mechanical tension, due to the constrained entropy, in the ribosome tunnel. The ability of TF to fold against the force generates mechanical power that pulls the polypeptide out of the ribosome. Other than assisting in folding process, TF carries its folded substrate to the SecA translocon motor, attached to the SecYEG translocon pore [34,46–48]. However, this TF presented polypeptide is not translocated by the SecA until it is unfolded by SecB, the go-to chaperone for translocation of several periplasmic proteins [26,34,46,49,50]. It is already reported that SecB binds to molten globule like structure of MBP [33], however, in equilibrium we found that SecB under mechanical constraints binds to unfolded state and reduces the proteins ability to work by half (Fig. 9C). This causes the reshaping of the energy landscape by stabilizing the unfolded state that requires almost 25 times more energy to fold into its native form. Interestingly, higher expression of DnaJ or DnaK compensates the absence of SecB in translocation of proteins identifying another pathway where these chaperones direct the specific client proteins to the SecA translocon motor [26]. In addition to their functional similarity with SecB, both DnaK and DnaJ individually prevent their substrate from folding, though their substrate specificity differs. Such as DnaK majorly binds to the molten globule state of mechanically stable ubiquitin while DnaJ binds to completely unfolded polypeptide chain [31]. However, both of them shift the energy landscape towards the unfolded state, which prevent the folding and letting the polyprotein to do minimum mechanical work (Fig. 9C). This makes sense as otherwise, if the protein gets folded by itself, its translocation through the SecYEG pore might get hampered due to the geometric constraints or excess energy might be needed by SecA or other unfoldases to disrupt the tertiary folded structure [5,33,48]. However, DnaJ and DnaK along with the GrpE makes the substrate folded by simply restoring its innate ability to refold under force, which has been clearly observed at equilibrium force condition (Fig 5). So, if the substrate is a cytosolic protein, it will be assisted by foldase like, TF and DnaKJE complex otherwise, periplasmic proteins will be assisted by unfoldase like SecB, DnaK or DnaJ till they interact with SecA motor. Once received by the SecA, it keeps translocating the substrate which either remains unfolded by themselves or kept unfolded by other unfoldases, through the SecYEG pore at 20 amino acids or > 125-250 amino acids per ATP hydrolysis cycle, according to the destination of the proteins [48,51]. In this translocon pore the unfolded polypeptide experiences the same force as they face in ribosomal tunnel, which makes them unable to fold till they get to the periplasmic side. In the periplasmic side of SecYEG, DsbA folds the polypeptide and fastens the pulling of protein out of the tunnel by increasing its refolding kinetics. This enables the protein folding to generate 1.6 times more mechanical work at 8 pN than in absence of DsbA.

This excess work done by the polyprotein folding accelerates its translocation, with reducing one-third of the energy consumed by SecA motor during usual translocation process (Fig. 10). In this whole protein folding pathway, our work provides the idea of how effectively the chaperones function by reducing the ATP consumption that makes the protein folding to produce more mechanical work. This directs an efficient energy partitioning mechanism to simultaneously carry out other cellular phenomena using the same amount of energy. Thus, these roles of chaperones in making their respective substrate to fold or unfold under force enable us to redefine them as the 'mechanical chaperones'.

Materials and Methods:

Purification and expression of protein L:

Sub-cloning of protein L construct were engineered using *Bam*HI, *Bgl*II and *Kpn*I restriction sites as described previously in [20]. A polyprotein was constructed by consecutively attaching eight protein L B1 domains, with a C-terminal AviTag for biotinylation and N-terminal Halo-Tag. This polyprotein construct was transformed into *Escherichia coli* BL21 (DE3 Invitrogen) competent cells. The cells were then grown in luria broth with carbenicillin for selection. After reaching optical density of 0.6- 0.8 at 600nm, cultures were induced with 1mM Isopropyl β-D-thiogalactopyranoside (IPTG, Sigma-Aldrich) and incubated overnight at 25^{o}C. The cells were pelleted at 8000rpm for 15 minutes and resuspended in 50mM sodium phosphate buffer pH 7.4 with 10% glycerol and 300mM NaCl. 10µM Phenylmethylsulfonyl (PMSF), as protease inhibitor, was added subsequently followed by lysozyme for membrane disruption. The dissolved pellet was ice incubated for 20minutes and mixed slowly at 4ºC. The solution was then treated with Triton-X 100 (Sigma-Aldrich), DNase, RNase (Invitrogen) and MgCl2 and mixed in rocking platform at 4^{o}C. The cells were homogenized at 19psi and the cell lysate was collected after centrifugation. The protein was purified using Ni^{2+}-NTA affinity chromatography of AKTA^{TM} Pure (GE healthcare). 20mM imidazole containing binding buffer was used for the proteins for attaching to the column which was later eluted by 250mM imidazole containing buffer. Biotinylation of polyprotein was done by Avidity biotinylation kit which was purified with Superdex-200 HR gel filtration column (GE healthcare) with 150mM NaCl containing buffer.

Expression and Purification of chaperons (DnaK, DnaJ, SecB, GrpE and DsbA):

Transforming the chaperone constructs in *Escherichia coli* DE3 cells (Invitrogen) provided us selected colonies which were then grown in luria broth media with respective antibiotics (ampicillin and carbenicillin 50ug/ml) at 37^{o} C. Cells were induced with 1mM Isopropyl β-D-

thiogalactopyranoside (IPTG, Sigma-Aldrich) and incubated overnight at 25^{o}C for harvesting. The cells were harvested by centrifugation and pellet was resuspended in phosphate buffer (pH 7.4) with 10% glycerol and 300 mM NaCl. The solution was then mixed at 4^{o} C with PMSF and lysozyme in it. Triton-X, DNase, RNase, and MgCl2 were added subsequently and mixed too. The cells were then burst open at 19psi using french press followed by collection of cell lysate and purification using Ni^{2+}-NTA affinity column of AKTA^{TM} Pure (GE Healthcare). The proteins were purified using 20mM imidazole containing binding buffer and 250mM imidazole containing elution sodium phosphate buffer (pH 7.4). Followed by purification the proteins were separated from salts and concentrated using Amicon Ultra 15 (Merck). In case of DsbA, after pelleting the cell at 8000 rpm it was collected in a pH 8.0, 50 mM Tris buffer with 20% (W/V) sucrose and 1mM EDTA. DNase, Rnase and PMSF were also added to this mixture followed by ice incubation. This resuspended solution was centrifuged where the supernatant (S-1) was collected while the pellet was dissolved in 20mM Tris solution. This mixture was again centrifuged and supernatant (S-2) was collected. The two supernatant containing protein lysate (S-1 and S-2) was purified by 1M NaCl containing Tris buffer using AKTA^{TM} Pure protein purification system with Hi-Trap Q-FF anion exchange column (GE healthcare). 0.3% H2O2 was added to the purified proteins. Further size exclusion purification was done with Superdex-200 HR column of GE healthcare, with a running buffer containing 150mM NaCl.

Preparation of glass slide and coverslips:

RT-MMT experiments was carried out in a microfluidic chamber by sandwiching a glass slide and a coverslip (top and bottom), separated with thin layer of paraflim, providing an inlet and outlet system. Initially, the glass slides were washed with 1.5% Hellmanex III solution (Sigma aldrich) and washed with double distilled water. The slides were then dipped in a solution containing methanol (CH_3OH) and hydrochloric acid (HCl) following which they were soaked with sulphuric acid (H_2SO_4) and then washed. The slides were then treated in boiling water and then dried. For activating the glass surface 1% (3-Aminopropyl) trimethoxysilane (sigma Aldrich, 281778) was dissolved in ethanol and was silanized for 15 minutes. To remove the unreacted silane the glasses were ethanol washed and the surfaces were then baked at 65^{o}C for ~ 2 hour. Top coverslips were cleaned with 1.5% Hellmanex III solution (Sigma aldrich) for 15 minutes and washed with ethanol followed by drying it in the oven for 10 minutes. The microfluidic chamber was then made by sandwiching the slide and coverslip, which was then filled with glutaraldehyde (Sigma Aldrich, G7776) in PBS buffer. After an hour, the chamber was washed with non-magnetic beads (2.5-2.9µm, Spherotech,

AP-25-10) reference beads followed by Halo-Tag amine (O_4) ligand (Promega, P6741). The chambers were then treated with a blocking buffer (20mM Tris-HCl, pH 7.4, 150mM NaCl, 2mM $MgCl_2$, 1% BSA, 0.03% NaN_3) to avoid non-specific interaction and kept in room temperature for 5 hours.

Real time multiplexed Microfluidic magnetic tweezers (RT-MMT) technology:

Real time multiplexed microfluidic magnetic tweezers was setup on an inverted microscope with an oil-immersion objective that remains attached to a nanofocusing piezo. The magnet position was controlled through the voice-coil, located just above the sample chamber. The sample chamber was viewed using a white LED and the diffraction pattern images were collected with ximea camera (MQ013MG-ON). Gaussian fits were applied to determine the absolute position and the required data, corresponding to each step, was calculated by length histograms. The changes in length between the centers of two histogram peaks denotes the step size. Detailed information regarding RT-MMT techniques and image processing are described in our previous article [12]. The magnetic tweezers experiment was carried out with 5 nM of protein L in a buffer containing 20mM sodium phosphate, 140 mM NaCl and 10mM ascorbic acid and pH of 6.8. After passing the protein L through the chamber the octamer was attached with a paramagnetic bead (Dynabeads M-270) to which the force is applied with a pair of neodymium magnets. We applied different forces to measure the step size, describing the unfolding and refolding of single protein domains. Different force was applied on protein L to which the effect of different chaperones was observed.

Acknowledgement:

We thank Ashoka University for support and funding. S.H. thanks DBT Ramalingaswami Fellowship and DST SERB Core Research Grant for funding. We thank Prof. Julio Fernandez (Columbia University) for helping us with the magnetic tweezers set up and Dr. Koyeli Mapa of Shiv Nadar University for kindly sharing with us the clones of SecB, DnaK, DnaJ, GrpE proteins. We thank Dr. Kausik Chakraborty (Institute of Genomics and Integrative Biology) and Prof. Gautam Menon (Ashoka University) for the critical analysis of the manuscript.

Conflict of Interest:

The authors declare no conflict of interest.

References:

1. Wruck, F., Katranidis, A., Nierhaus, K. H., Büldt, G. & Hegner, M. Translation and folding of single proteins in real time. *Proc. Natl. Acad. Sci.* **114**, E4399–E4407 (2017).

2. Maillard, R. A. *et al.* ClpX(P) generates mechanical force to unfold and translocate its protein substrates. *Cell* (2011). doi:10.1016/j.cell.2011.04.010

3. Rivas-Pardo, J. A. *et al.* Work Done by Titin Protein Folding Assists Muscle Contraction. *Cell Rep.* **14**, 1339–1347 (2016).

4. Eckels, E. C., Tapia-Rojo, R., Rivas-Pardo, J. A. & Fernández, J. M. The Work of Titin Protein Folding as a Major Driver in Muscle Contraction. *Annu. Rev. Physiol.* **80**, 327–351 (2018).

5. Gupta, R., Toptygin, D. & Kaiser, C. M. The SecA motor generates mechanical force during protein translocation. *Nat. Commun.* **11**, 3802 (2020).

6. Goldman, D. H. *et al.* Mechanical force releases nascent chain-mediated ribosome arrest in vitro and in vivo. *Science (80-.).* **348**, 457–460 (2015).

7. Hartl, F. U. Molecular chaperones in cellular protein folding. *Nature* **381**, 571–9 (1996).

8. Hartl, F. U., Bracher, A. & Hayer-Hartl, M. Molecular chaperones in protein folding and proteostasis. *Nature* **475**, 324–332 (2011).

9. Hartl, F. U. Molecular Chaperones in the Cytosol: from Nascent Chain to Folded Protein. *Science (80-.).* **295**, 1852–1858 (2002).

10. Walter, S. & Buchner, J. Molecular Chaperones—Cellular Machines for Protein Folding. *Angew. Chemie Int. Ed.* **41**, 1098–1113 (2002).

11. Kim, Y. E., Hipp, M. S., Bracher, A., Hayer-Hartl, M. & Hartl, F. U. Molecular chaperone functions in protein folding and proteostasis. *Annu. Rev. Biochem.* **82**, 323–55 (2013).

12. Chakraborty, S. *et al.* Real-Time Microfluidics-Magnetic Tweezers connects conformational stiffness with energy landscape by a single experiment. *bioRxiv*

2020.06.09.142257 (2020). doi:10.1101/2020.06.09.142257

13. Haldar, S., Tapia-Rojo, R., Eckels, E. C., Valle-Orero, J. & Fernandez, J. M. Trigger factor chaperone acts as a mechanical foldase. *Nat. Commun.* **8**, 668 (2017).

14. Agashe, V. R. *et al.* Function of trigger factor and DnaK in multidomain protein folding: Increase in yield at the expense of folding speed. *Cell* (2004). doi:10.1016/S0092-8674(04)00299-5

15. Imamoglu, R., Balchin, D., Hayer-Hartl, M. & Hartl, F. U. Bacterial Hsp70 resolves misfolded states and accelerates productive folding of a multi-domain protein. *Nat. Commun.* **11**, 365 (2020).

16. Nunes, J. M., Mayer-Hartl, M., Hartl, F. U. & Müller, D. J. Action of the Hsp70 chaperone system observed with single proteins. *Nat. Commun.* **6**, 6307 (2015).

17. Szabo, A. *et al.* The ATP hydrolysis-dependent reaction cycle of the Escherichia coli Hsp70 system DnaK, DnaJ, and GrpE. *Proc. Natl. Acad. Sci. U. S. A.* **91**, 10345–9 (1994).

18. Clerico, E. M., Tilitsky, J. M., Meng, W. & Gierasch, L. M. How hsp70 molecular machines interact with their substrates to mediate diverse physiological functions. *J. Mol. Biol.* **427**, 1575–88 (2015).

19. Mayer, M. P. Hsp70 chaperone dynamics and molecular mechanism. *Trends Biochem. Sci.* **38**, 507–514 (2013).

20. Popa, I. *et al.* A HaloTag Anchored Ruler for Week-Long Studies of Protein Dynamics. *J. Am. Chem. Soc.* **138**, 10546–10553 (2016).

21. Szabo, A., Korszun, R., Hartl, F. U. & Flanagan, J. A zinc finger-like domain of the molecular chaperone DnaJ is involved in binding to denatured protein substrates. *EMBO J.* **15**, 408–17 (1996).

22. Schröder, H., Langer, T., Hartl, F. U. & Bukau, B. DnaK, DnaJ and GrpE form a cellular chaperone machinery capable of repairing heat-induced protein damage. *EMBO J.* **12**, 4137–44 (1993).

23. Plaxco, K. W., Millett, I. S., Segel, D. J., Doniach, S. & Baker, D. Chain collapse can

occur concomitantly with the rate-limiting step in protein folding. *Nat. Struct. Biol.* **6**, 554–6 (1999).

24. Scalley, M. L. *et al.* Kinetics of folding of the IgG binding domain of peptostreptococcal protein L. *Biochemistry* **36**, 3373–82 (1997).

25. Yi, Q., Scalley-Kim, M. L., Alm, E. J. & Baker, D. NMR characterization of residual structure in the denatured state of protein L. *J. Mol. Biol.* **299**, 1341–1351 (2000).

26. Wild, J., Altman, E., Yura, T. & Gross, C. A. DnaK and DnaJ heat shock proteins participate in protein export in Escherichia coli. *Genes Dev.* **6**, 1165–72 (1992).

27. Langer, T. *et al.* Successive action of DnaK, DnaJ and GroEL along the pathway of chaperone-mediated protein folding. *Nature* (1992). doi:10.1038/356683a0

28. Kityk, R., Kopp, J., Sinning, I. & Mayer, M. P. Structure and Dynamics of the ATP-Bound Open Conformation of Hsp70 Chaperones. *Mol. Cell* **48**, 863–874 (2012).

29. Mashaghi, A. *et al.* Alternative modes of client binding enable functional plasticity of Hsp70. *Nature* (2016). doi:10.1038/nature20137

30. Balchin, D., Hayer-Hartl, M. & Hartl, F. U. In vivo aspects of protein folding and quality control. *Science (80-.).* **353**, aac4354 (2016).

31. Perales-Calvo, J., Giganti, D., Stirnemann, G. & Garcia-Manyes, S. The force-dependent mechanism of DnaK-mediated mechanical folding. *Sci. Adv.* **4**, eaaq0243 (2018).

32. Zhuravleva, A. & Gierasch, L. M. Substrate-binding domain conformational dynamics mediate Hsp70 allostery. *Proc. Natl. Acad. Sci.* **112**, E2865–E2873 (2015).

33. Bechtluft, P. *et al.* Direct observation of chaperone-induced changes in a protein folding pathway. *Science (80-.).* (2007). doi:10.1126/science.1144972

34. Bechtluft, P., Nouwen, N., Tans, S. J. & Driessen, A. J. M. SecB—A chaperone dedicated to protein translocation. *Mol. BioSyst.* **6**, 620–627 (2010).

35. Alonso-Caballero, A. *et al.* Mechanical architecture and folding of E. coli type 1 pilus domains. *Nat. Commun.* (2018). doi:10.1038/s41467-018-05107-6

36. Haldar, S., Eckels, E. C., Echelman, D. J., Rivas-Pardo, J. A. & Fernandez, J. M. DsbA is a switchable mechanical chaperone. *bioRxiv* (2018).

37. Pan, J. L. & Bardwell, J. C. A. The origami of thioredoxin-like folds. *Protein Sci.* **15**, 2217–2227 (2006).

38. Duprez, W. *et al.* Peptide Inhibitors of the Escherichia coli DsbA Oxidative Machinery Essential for Bacterial Virulence. *J. Med. Chem.* **58**, 577–587 (2015).

39. Kurth, F. *et al.* Crystal structure of the dithiol oxidase DsbA enzyme from proteus mirabilis bound non-covalently to an active site peptide ligand. *J. Biol. Chem.* **289**, 19810–22 (2014).

40. Sauvonnet, N. & Pugsley, A. P. The requirement for DsbA in pullulanase secretion is independent of disulphide bond formation in the enzyme. *Mol. Microbiol.* **27**, 661–7 (1998).

41. Javadi, Y., Fernandez, J. M. & Perez-Jimenez, R. Protein folding under mechanical forces: A physiological view. *Physiology* (2013). doi:10.1152/physiol.00017.2012

42. Eckels, E. C., Haldar, S., Tapia-Rojo, R., Rivas-Pardo, J. A. & Fernández, J. M. The Mechanical Power of Titin Folding. *Cell Rep.* (2019). doi:10.1016/j.celrep.2019.04.046

43. Olivares, A. O., Baker, T. A. & Sauer, R. T. Mechanical Protein Unfolding and Degradation. *Annu. Rev. Physiol.* **80**, 413–429 (2018).

44. Popa, I. & Berkovich, R. Mechanobiology: protein refolding under force. *Emerg. Top. Life Sci.* (2018). doi:10.1042/etls20180044

45. Alder, N. N. & Theg, S. M. Energy use by biological protein transport pathways. *Trends Biochem. Sci.* **28**, 442–451 (2003).

46. De Geyter, J. *et al.* Trigger factor is a bona fide secretory pathway chaperone that interacts with SecB and the translocase. *EMBO Rep.* **21**, e49054 (2020).

47. Kusters, I. & Driessen, A. J. M. SecA, a remarkable nanomachine. *Cell. Mol. Life Sci.* **68**, 2053–66 (2011).

48. Cranford-Smith, T. & Huber, D. The way is the goal: how SecA transports proteins

across the cytoplasmic membrane in bacteria. *FEMS Microbiol. Lett.* **365**, (2018).

49. Ullers, R. S. *et al.* SecB is a bona fide generalized chaperone in Escherichia coli. *Proc. Natl. Acad. Sci. U. S. A.* **101**, 7583–8 (2004).

50. Sala, A., Bordes, P. & Genevaux, P. Multitasking SecB chaperones in bacteria. *Front. Microbiol.* **5**, (2014).

51. Schiebel, E., Driessen, A. J. M., Hartl, F. U. & Wickner, W. ΔμH+ and ATP function at different steps of the catalytic cycle of preprotein translocase. *Cell* (1991). doi:10.1016/0092-8674(91)90317-R

Figures

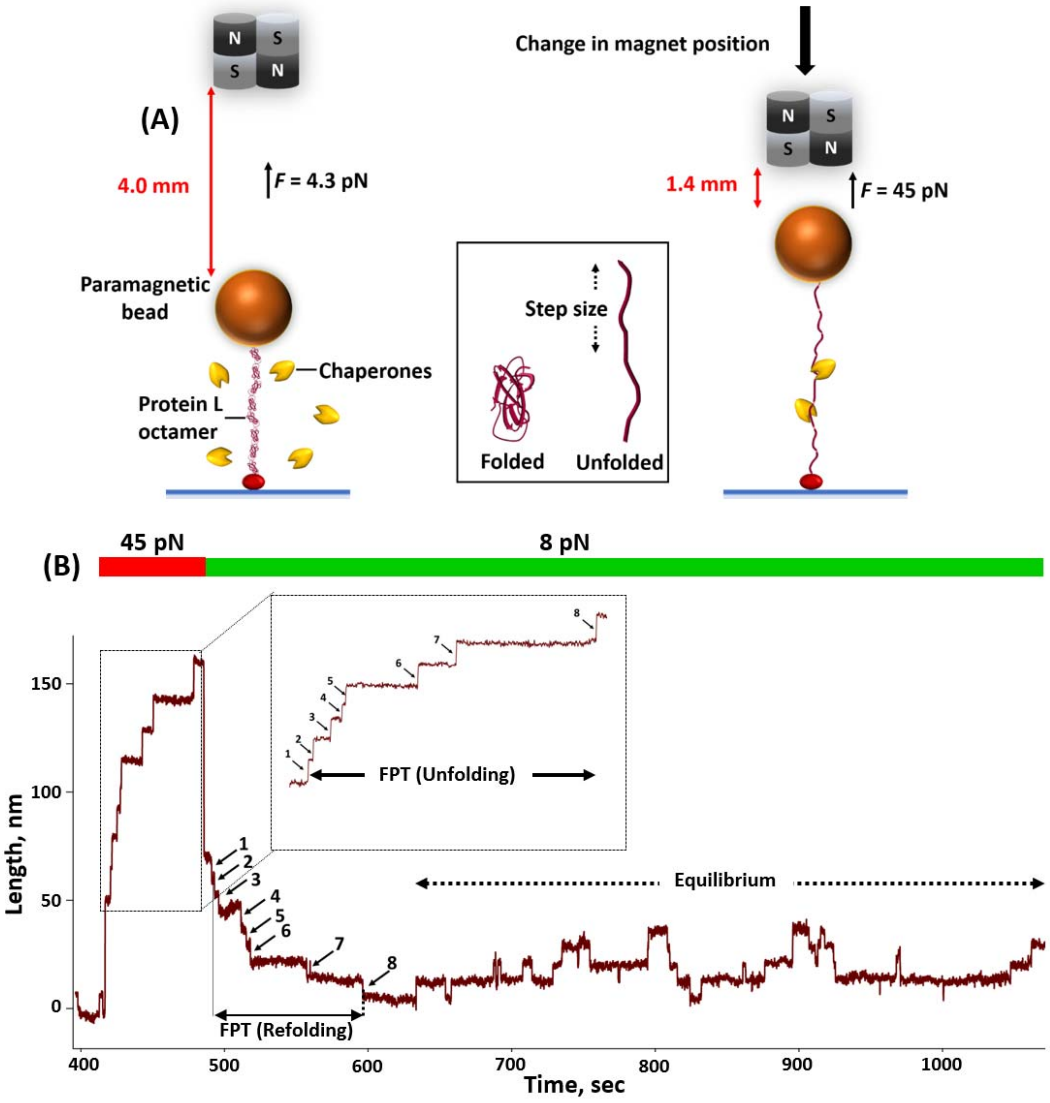

Figure 1: Experimental set-up for real-time microfluidic-magnetic tweezers (RT-MMT) to study protein-chaperone interaction: (A) Schematics of RT-MMT experiment: *The engineered construct of eight identical protein L domain, inserted between N terminus HaloTag for attaching to ligand coated glass surface and C terminus AviTag for binding to streptavidin coated paramagnetic beads. Applied force is controlled by changing the distance between permanent magnet and paramagnetic beads. The distance between folded and unfolded state is denoted as step-size.* ***(B) Standard folding trajectory of protein L octamer:*** *First, the polyprotein is unfolded at high force pulse of 45 pN, generating eight successive*

steps as single molecule fingerprint that followed by a refolding pulse at 7 pN. During refolding, the polyprotein first undergoes a relaxation phase followed by an equilibrium phase where the domains show a continuous hopping between folded and unfolded state. The duration of complete unfolding from fully folded state is called first passage time (FPT) of unfolding and the time taken to achieve complete refolding from fully unfolded state is called FPT of refolding.

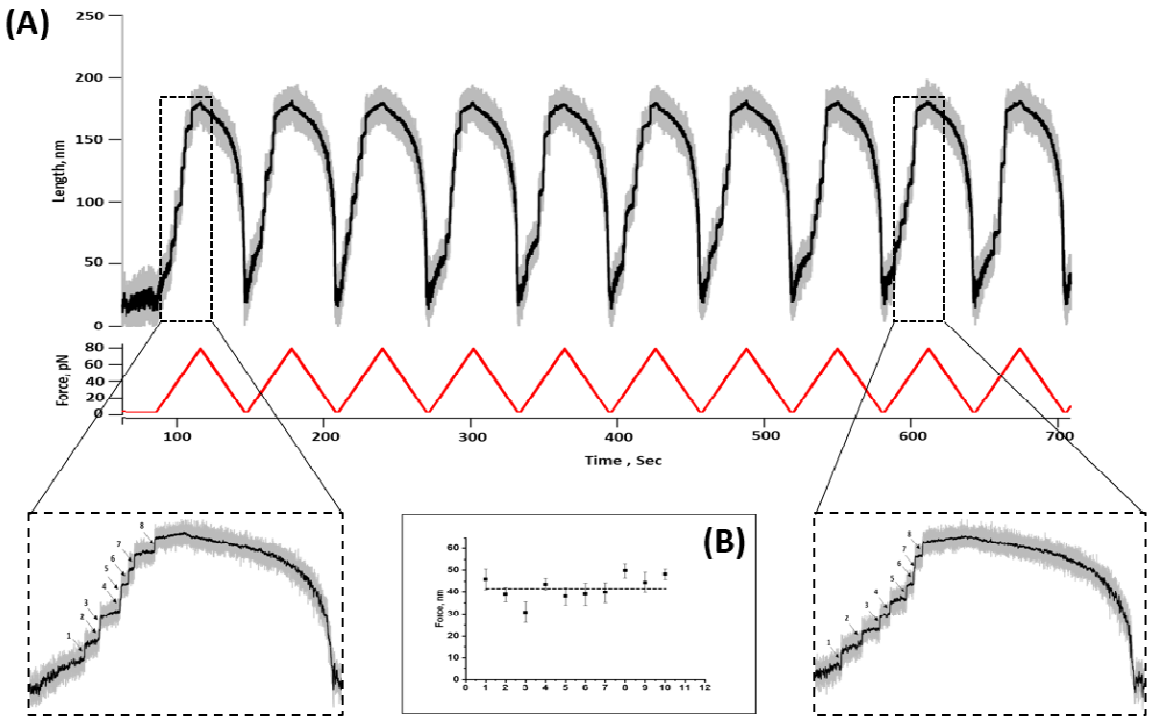

Figure 2: Mechanical strength of protein L octamer: (A) Force ramp study: *Successive force ramp, from 4 to 80 pN at 2.53pN/s ramp rate, are applied to detect the presence of any misfolded states. The unfolding traces are magnified to observe eight discrete step sizes throughout the successive ramp study.* ***(B)Mechanical strength of proteinL does not change with unfolding/refolding pulses:*** *Mechanical strength of polyprotein does not change with unfolding and refolding pulses, showing the absence of any misfolded state of proteinL under force.*

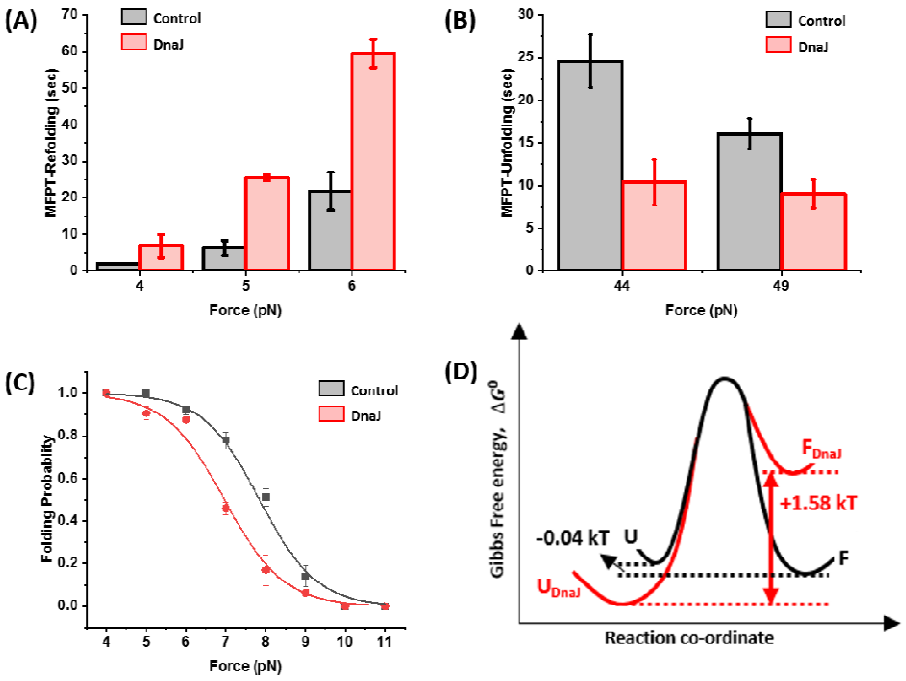

Figure 3: DnaJ negatively modulates the folding events in protein L: ***(A) Variation in MFPT of refolding in absence (black) and presence of DnaJ (red):*** *MFPT values are plotted as a function of force in absence (black) and presence of DnaJ (red). In the presence of DnaJ, the MFPT of refolding is higher than in absence of DnaJ.* ***(B) Variation in MFPT of unfolding:*** *Addition of DnaJ reduces the MFPT of unfolding at a constant force, indicating faster unfolding kinetics.* ***(C) Folding probability in absence (black) and presence of DnaJ (red):*** *The presence of molecular chaperone DnaJ reduces the folding probability within the range of 5-9 pN force. Accordingly, half point force is also shifted from 8 pN to 6.94 pN, suggesting a pronounced reduction in folding probability in the presence of DnaJ.* ***(D) Reshaping the energy landscape:*** *DnaJ reshapes the energy landscape towards the unfolded state by destabilizing the folded state while keeping the unfolded state stable.*

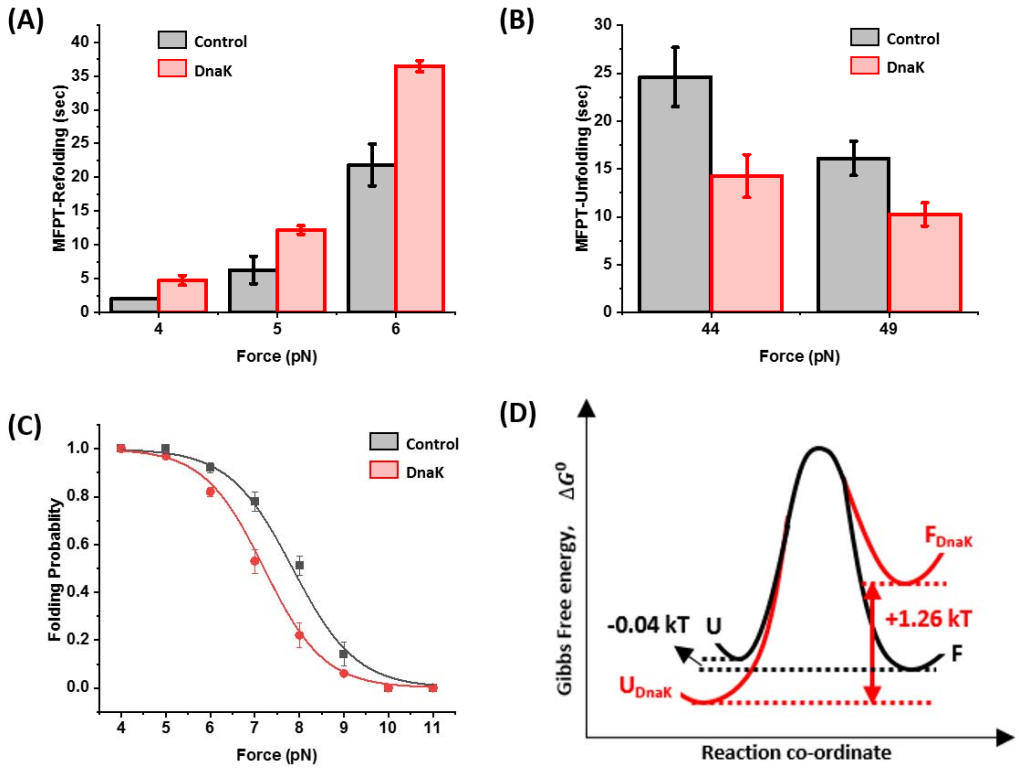

Figure 4: The effect of DnaK on protein folding events: (A) Comparison in MFPT of refolding: *MFPT values are plotted as a function of force in absence (black) and presence of DnaK (red). At a particular force in presence of DnaK, the MFPT refolding is higher than in absence of DnaK.* ***(B) Comparison in MFPT of unfolding:*** *DnaK (red) accelerates the unfolding kinetics almost two-fold than in absence of DnaK (black).* ***(C)Folding Probability:*** *The folding probability is plotted as a function of force in absence (black) and presence of DnaK (red). The presence of DnaK substantially decreases the folding probability at a particular force and thus, the half-point force is shifted from 8 pN to 7.18 pN.* ***(D) Energy landscape:*** *DnaK inclines the energy landscape towards the unfolded state by destabilizing the folded state and stabilizing the unfolded state.*

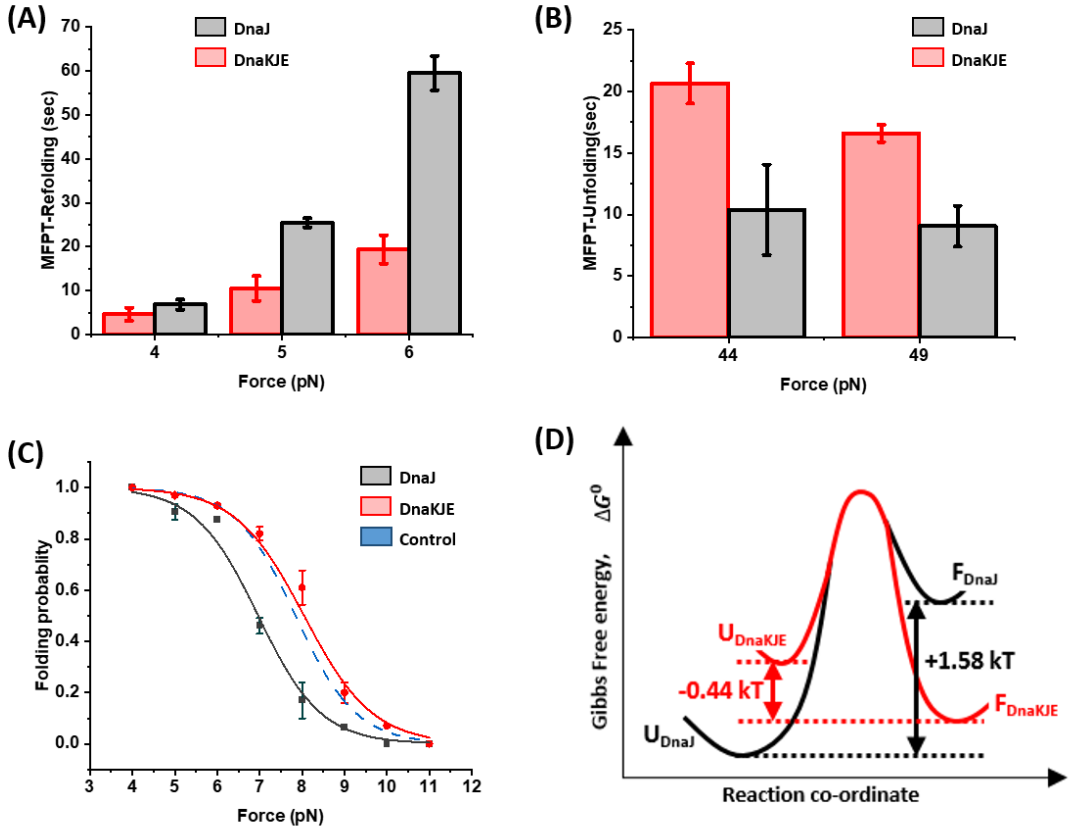

Figure 5: DnaKJE chaperone complex restores the folding ability in protein L: (A) Differences in MFPT of refolding: *MFPT of refolding is plotted as a function of force with DnaJ (black) and DnaK chaperone complex (red). ProteinL shows lower refolding time in the presence of DnaKJE complex (red) than in presence of DnaJ (black).* ***(B) Differences in MFPT of unfolding:*** *Presence of whole chaperone system (red) increases the total unfolding time than only DnaJ. At 44 pN, the proteinL requires 10.38±3.67 s to complete unfold in presence of DnaJ (black) while it reaches to 20.63±1.63 s in presence of DnaKJE (red).* ***(C)Comparison of folding Probability:*** *Folding probabilities with DnaJ (black) and chaperone system (red) are plotted within 4-11 pN range where it has been shown to substantially increase the folding probability than DnaJ over the 5-9 pN force range.* ***(D) Effect on energy landscape:*** *DnaKJE reverts the energy landscape towards folded state by stabilizing the folded state and destabilizing the unfolded state.*

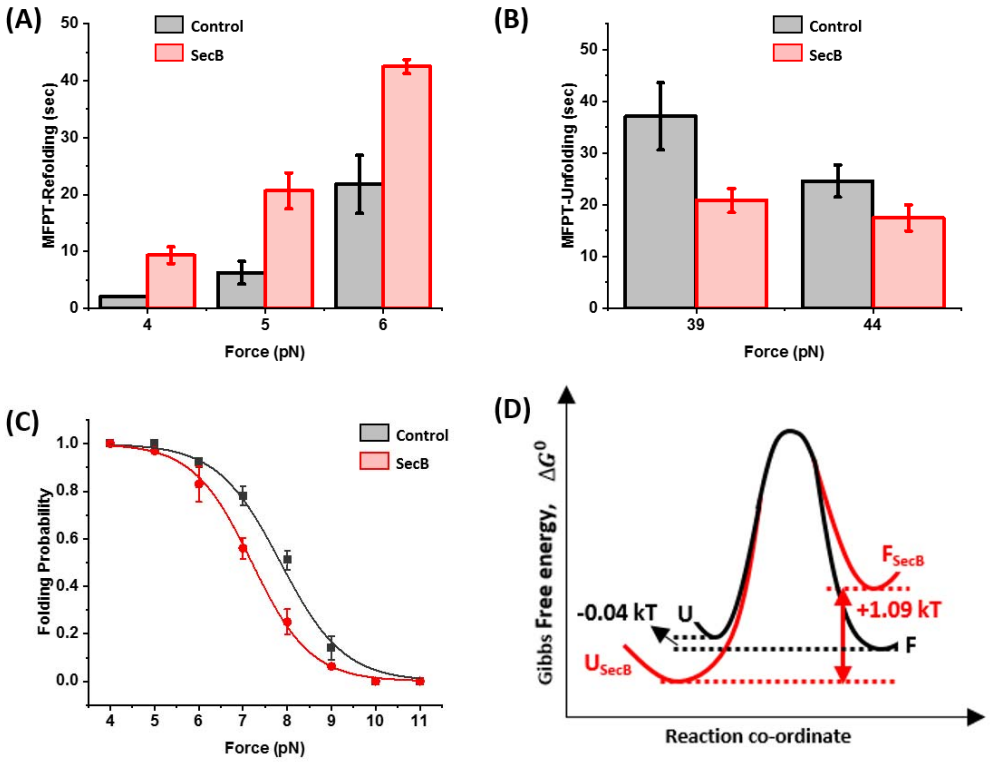

Figure 6: SecB dependency of folding properties of protein L: (A) MFPT of refolding: *SecB decreases the refolding kinetics of proteinL at a particular force. MFPT refolding is higher in presence of SecB (red) in comparison to control (black).* ***(B) MFPT of unfolding:*** *SecB increases the unfolding kinetics at a constant force. MFPT unfolding is lower in presence of SecB (red) in comparison to control (black).* ***(C) Folding properties:*** *SecB reduces the folding probability as a particular force and the half-point force is also reduced from 8 pN to 7.17 pN suggesting a 50% reduction in folding probability.* ***(D) Effects on ΔG:*** *SecB tilts the energy landscape towards the unfolded state by destabilizing the folded state while keeping the unfolded state stable.*

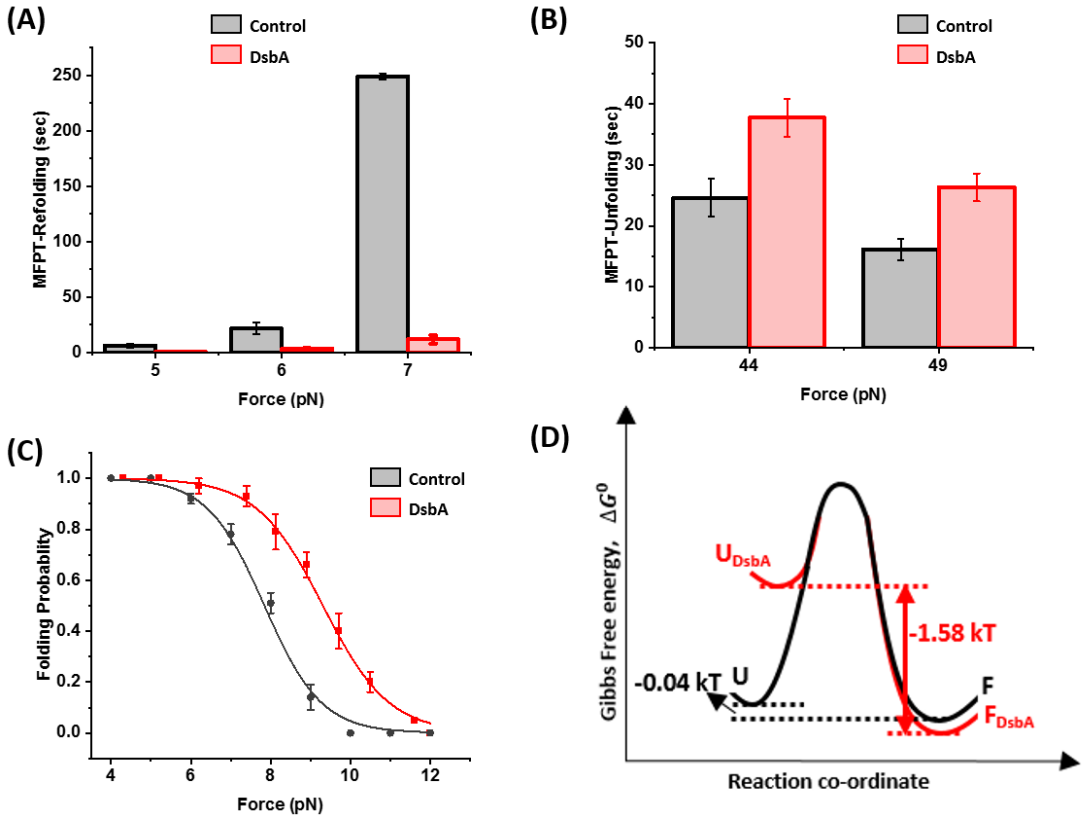

Figure 7: DsbA dependency of folding properties of protein L: (A) MFPT of refolding: *DsbA positively modulates the refolding kinetics by speeding up the time to refold all the eight domains. MFPT refolding is much lower in presence of DsbA (red) in comparison to control (black).* ***(B) MFPT of unfolding:*** *DsbA slightly changes the unfolding kinetics.* ***(C) Folding efficiency:*** *DsbA greatly increases the folding probability and the observed effect is most profound at 9 pN force. Folding probability of protein L in presence of DsbA shown in red, whereas in absence of DsbA shown in black.* ***(D) Effect on folding landscape:*** *DsbA tilts the folding landscape towards the folded state by destabilizing the unfolded state while slightly stabilizing the folded state.*

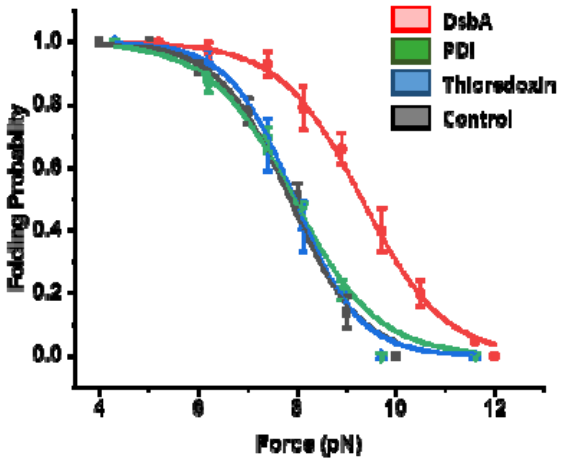

Figure 8: Comparison in folding probability of different thioredoxin domain containing proteins: *Folding probability of proteinL is plotted against force in presence of full length PDI (green), Trx (blue) and DsbA (Red). Full length PDI and Trx, being cytosolic thioredoxin domain containing proteins, have only been observed to restore the folding efficiency in protein and overlaps with folding probability in control, whereas the tunnel associated counterpart DsbA not only restores but also accelerate the refolding yield in proteins under force. For example, at 8 pN, in presence of PDI and Trx, the folding probabilities are 0.49 and 0.45, respectively while it increases to 0.83 in presence of DsbA.*

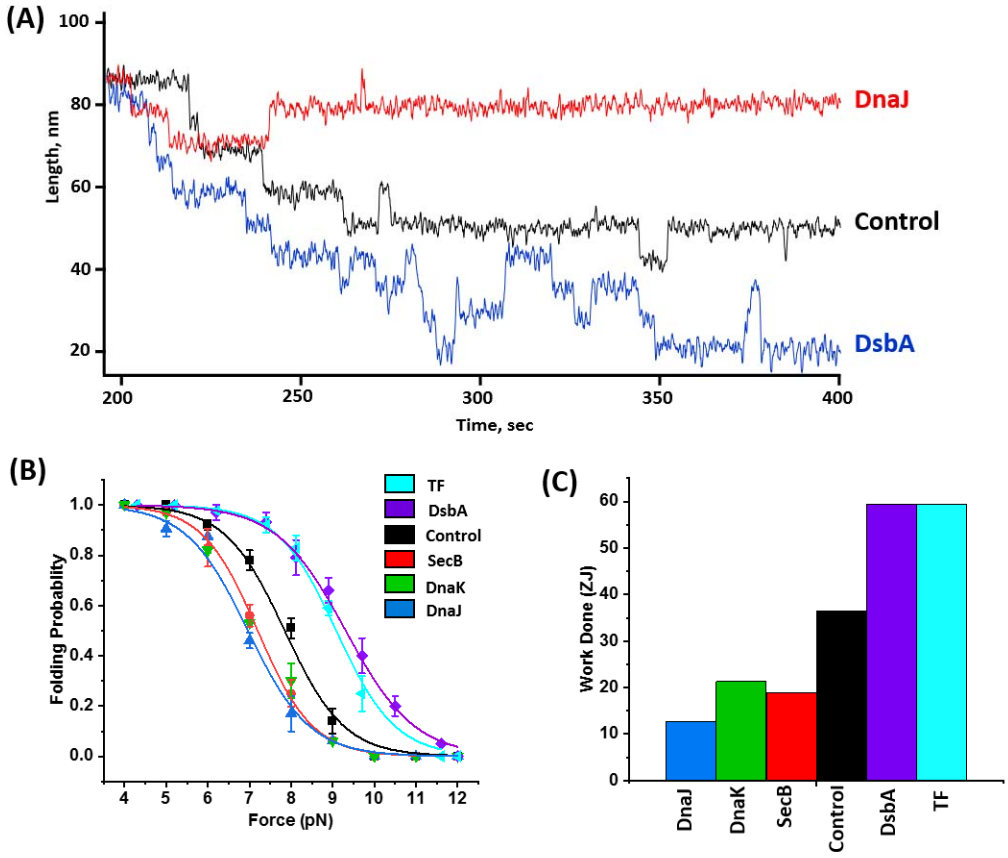

Figure 9: Mechanical activity of different chaperone under equilibrium force condition: ***(A) Comparisons in folding transitions in presence of different chaperones:*** *In absence of any chaperones (control, black trace), the polyprotein hops between its 4th and 5th folded state while introducing chaperones shift this folding transitions either towards folded state (downward) or unfolded (upward) state. For example, in the presence of DnaJ (red trace) proteinL show a folding transition between its 1st and 2nd folded states while addition of DsbA (blue trace), increases this intrinsic folding ability, allowing a folding-unfolding transition between the 6th, 7th and 8th folded states.* ***(B) Variation in folding probability:*** *Folding probability is plotted against the force with different chaperones. In presence of DsbA and TF, the folding probability is shifted rightward, suggesting a higher folding probability whereas the presence of chaperones such as, DnaJ, DnaK, and SecB retards the folding probability, representing a compromised refolding yield.* ***(C) Mechanical work output of different chaperones:*** *Mechanical work output is determined as the product of force, step size at that force and the folding probability. The calculated mechanical work for different chaperones are plotted where it has been observed that foldase like, TF and DsbA*

generate 59.5 zJ mechanical work where unfoldase such as, DnaJ, DnaK, and SecB generate 12.71, 21.36 and 18.94 zJ, respectively.

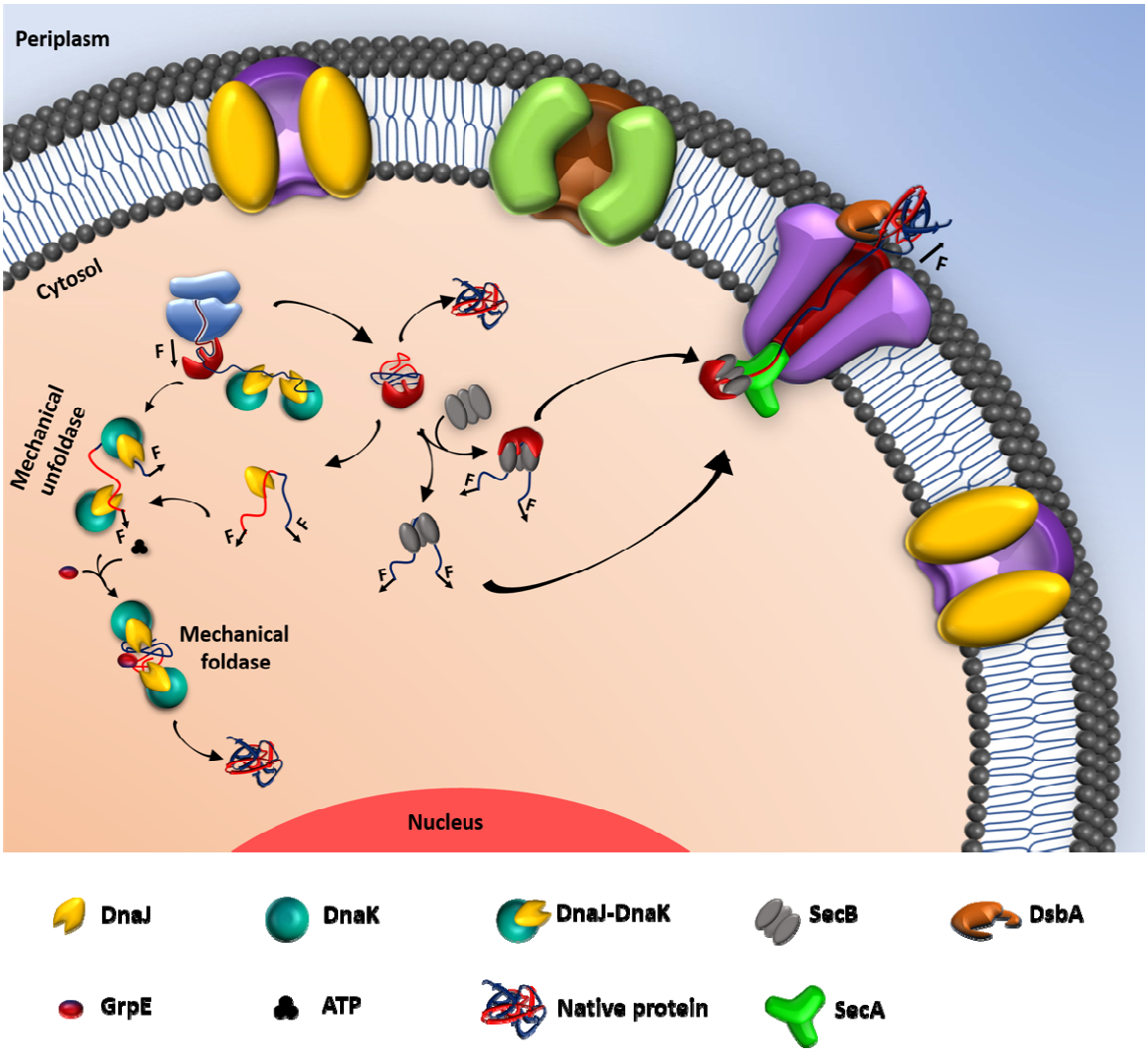

Figure 10: Chaperone mediated folding pathway: *Trigger Factor is the first chaperone to interact with the nascent polypeptide, emerging from the ribosome and in majority cases, the newly synthesized polypeptide chain natively fold without further assistance. Otherwise, nascent chains can co- or post-transnationally interact with DnaJ-DnaK chaperones and GrpE to achieve their proper folding. Here, DnaJ and DnaK act as mechanical unfoldase that mechanically unfolds the client proteins while a further assistance of GrpE helps the complex to function as mechanical foldase where they synergistically restore the protein folding ability under force. In a different pathway, TF, bound to the nascent chain, associates with SecB and helps the polypeptide in recruiting to SecA motor. SecB also has the ability to act as mechanical unfoldase by maintaining the unfolded state of the client protein to prevent premature misfolding. The unfolded polypeptide can be translocated through the SecYEG*

translocon pore where the periplasmic oxidoreductase DsbA increases the refolding yield under force.